Atmospheric and Oceanic Science Letters

ISSN: 1674-2834 (Print) 2376-6123 (Online) Journal homepage: https://www.tandfonline.com/loi/taos20

Extended-range prediction of a heat wave event over the Yangtze River Valley: role of intraseasonal signals

Xin QI & Jing YANG

To cite this article: Xin QI & Jing YANG (2019) Extended-range prediction of a heat wave event over the Yangtze River Valley: role of intraseasonal signals, Atmospheric and Oceanic Science Letters, 12:6, 451-457, DOI: 10.1080/16742834.2019.1669408

To link to this article: https://doi.org/10.1080/16742834.2019.1669408

Published online: 25 Sep 2019.

ATMOSPHERIC AND OCEANIC SCIENCE LETTERS
2019, VOL. 12, NO. 6, 451–457
https://doi.org/10.1080/16742834.2019.1669408

Extended-range prediction of a heat wave event over the Yangtze River Valley: role of intraseasonal signals

QI Xin[a] and YANG Jing[a,b]

[a]Key Laboratory of Environmental Change and Natural Disaster/Academy of Disaster Reduction and Emergency Management, Faculty of Geographical Science, Beijing Normal University, Beijing, China; [b]State Key Laboratory of Earth Surface Processes and Resource Ecology, Beijing Normal University, Beijing, China

ABSTRACT

The authors previous study reported the important role of extratropical intraseasonal oscillation (ISO) on the occurrence of a typical heatwave event over the Yangtze River Valley. Based on the ECMWF subseasonal reforecast database, this follow-up study evaluates the extended-range prediction skill of the heatwave event and further unravels the close link between the ISO and extended-range prediction of the event. With a two-week lead time, this heatwave event fails to occur in the reforecast because the predicted surface temperature is significantly underestimated. More detailed analysis demonstrates that the biases for both the intensity and the location of the warming region are primarily attributable to the inaccurate extratropical intraseasonal traveling signals. This work strongly indicates that accurately capturing the extratropical intraseasonal signal from the Eurasian continent is indispensable for extended-range prediction of East Asian extreme heatwave events.

摘要

江淮流域热浪事件的触发与大气季节内信号的传播密切相关。基于ECMWF次季节预测系统的回报数据，本研究在延伸期（10–30天）尺度上评估了一次典型江淮热浪事件的预测情况。评估采用气候态与季节内模态剥离的方法，揭示出大气季节内信号在江淮热浪延伸期预测中的必要作用。结果表明，相较于热带季节内信号，中纬度季节内信号在延伸期的预测偏差，是导致热浪超前2周预测失败的主要原因。本研究的重要启示是，提高中纬度地区大气季节内信号在延伸期尺度上的预测效果是提升东亚极端热浪事件预测水平的重要途径。

ARTICLE HISTORY
Received 5 April 2019
Revised 5 May 2019
Accepted 12 June 2019

KEYWORDS
Extended-range prediction; heat wave; intraseasonal perturbation; Yangtze River Valley

1. Introduction

Heatwaves pose serious risks socioeconomically and to public health in densely populated areas. Previous studies have found that most heatwave events over the Yangtze River Valley (YRV)—the core region of heatwave occurrence in eastern China—are closely related to the propagating intraseasonal oscillations (ISOs) from both the tropics and mid-to-high latitudes (Chen and Zhai 2017; Hsu et al. 2017; Gao et al. 2018). For instance, based on observational diagnostics, Chen, Wen, and Lu (2018) reported that the different ISO modes from the tropical western Pacific play distinct roles in different stages of long-lived extreme heat events, and our prior study (Qi et al. 2019) investigated the important role of intraseasonal perturbations from the extratropical region on heatwave generation using numerical experiments.

Given the frequent threat of heatwave events over the YRV, there is a growing demand for skillful heatwave prediction at the extended-range timescales (10–30 days). Several previous studies have attempted to predict heatwaves using statistical methods. For example, Teng et al. (2013) identified a pattern of anomalous atmospheric planetary wave trains with a wavenumber five at 15–20 days before the occurrence of heatwave events, but it is difficult to provide accurate information on upcoming heatwaves in terms of their start date, intensity, duration, and life cycle. Another spatiotemporal projection model (Zhu and Li 2018) can only predict about 30% of heatwave events within a 15-day lead time. The above disadvantages of statistical methods could be overcome by the dynamical prediction approach, because current dynamical models have exhibited better prediction skill owing to the development of high-performance computing and dynamic parameterization schemes (Mariotti, Ruti, and Rixen 2018). The subseasonal-to-seasonal (S2S) prediction project, jointly launched by the World Weather Research Program and the World Climate Research Program, has released a multi-model database of subseasonal forecasts/reforecasts (Vitart et al. 2017), which has provided new opportunities to investigate heatwave prediction at extended-range time scales.

CONTACT Jing YANG yangjing@bnu.edu.cn

Considering the crucial role played by ISOs in the occurrence of heatwaves over the YRV, the relationship between intraseasonal signals and the occurrence of heatwaves needs to be clarified from the viewpoint of extended-range prediction. In other words, does ISO play an important role in extended-range prediction of heatwave events? To answer this question, in the present study, the extended-range prediction of a typical heatwave event associated with ISO is comprehensively evaluated using the S2S database, and the influence of ISO prediction on heatwave generation is examined at the extended-range time scale.

2. Data and methods

The observed temperature data, with a 0.25° horizontal resolution, are from the CN05.1 dataset provided by the National Climate Center of China, and include the daily mean temperature at 2 m (T_m) and daily maximum temperature (T_{max}) (Xu et al. 2009; Wu and Gao 2013). The ECMWF's ERA-Interim datasets, on grids of 0.75° × 0.75°, are used to characterize the atmospheric circulation (Simmons et al. 2007; Dee et al. 2011). The ECMWF reforecasts, used to estimate the extended-range prediction skill, are from the World Meteorological Organization's S2S Prediction Project database. Note that the ECMWF S2S prediction system initialized a 10-member ensemble reforecast twice weekly for the 20-year period of 1995–2014 (Vitart et al. 2017), and here the ensemble mean is calculated to denote the results of the extended-range prediction.

In this study, the heatwave definition is for the target domain. Hence, the area-average T_m and T_{max} are first calculated over the YRV (26–33°N, 111–118°E), which are then applied to identify specific dates of heatwave events according to both the relative and absolute criteria as follows: (1) two consecutive days with T_m exceeding the 95th percentile of the daily climatology (defined over 1995–2014) (Anderson and Bell 2011); (2) three consecutive days with T_{max} exceeding 35°C (Huang, Kan, and Kovats 2010).

The ISO components for both the observation and reforecast are calculated from the raw daily temperature and circulation variables at each grid cell by first removing their own climatology and then removing synoptic fluctuations by taking a five-day running mean (Yang, Wang, and Bao 2010; Yang et al. 2014). The climatological daily mean data here are averaged in a leave-one-year-out manner, i.e. the climatology for a given year only considers the remaining 19 years.

3. Results

According to our recent study (Qi et al. 2019), the occurrence of the heatwave event over the YRV in summer 2012 was directly caused by a local strong high-pressure anomaly, which was generated by tropical–extratropical interaction of intraseasonal transient waves. Specifically, a westward tropical meridional dipole anomaly dominantly generated a lower-level anomalous anticyclone over the YRV during the early period of heatwave development, while the invasion of extratropical ISO contributed to the formation of a strong high-pressure anomaly during the late period of heatwave development, which together eventually caused the heatwave occurrence. To further verify the role played by the remotely propagating intraseasonal perturbations in the occurrence of this heatwave event, we examine the ECMWF reforecast of the event and investigate if the intraseasonal waves had an impact on the extended-range prediction. Here, the results with a two-week lead time are shown, but the main results reported below can also be seen well at a three-week lead.

3.1 Performance of the extended-range prediction for the heatwave event

As the observational data in Figure 1(a) show, the warming process started on 27 June and lasted nearly two weeks that concurrently belonged to a developing phase of the local ISO. According to the heatwave criteria, this event appeared during 9–12 July, which was in the peak warm stage of the local ISO (i.e. phase 5 in Figure 1(g)). By contrast, in the two-week-lead reforecast, the heatwave does not occur, because the warming amplitude measured by T_m is underestimated by almost 2°C. In terms of the heatwave spatial distribution shown in Figure 1(b,c), the warming maximum center shifts significantly northward in the two-week-lead reforecast compared with the observation. The maximum high temperature region (> 30°C), is mainly located in the south of the YRV (26°–30°N, 111–118°E) in the observation, but shifts to over the Yellow River Valley (33°–36°N) in the reforecast. Accordingly, the reforecast temperature during the observed heatwave period is much lower over the YRV.

We first examine whether the underestimation of the warming amplitude is caused by the reforecast climatological cooling bias. However, rather than cooling, the climatological reforecast bias shows evident warming by 1.1°C during the target period (the observed heatwave period) over the YRV (Figure 1(e,f)). Therefore, the cooling biases of the heatwave sub-seasonal reforecast

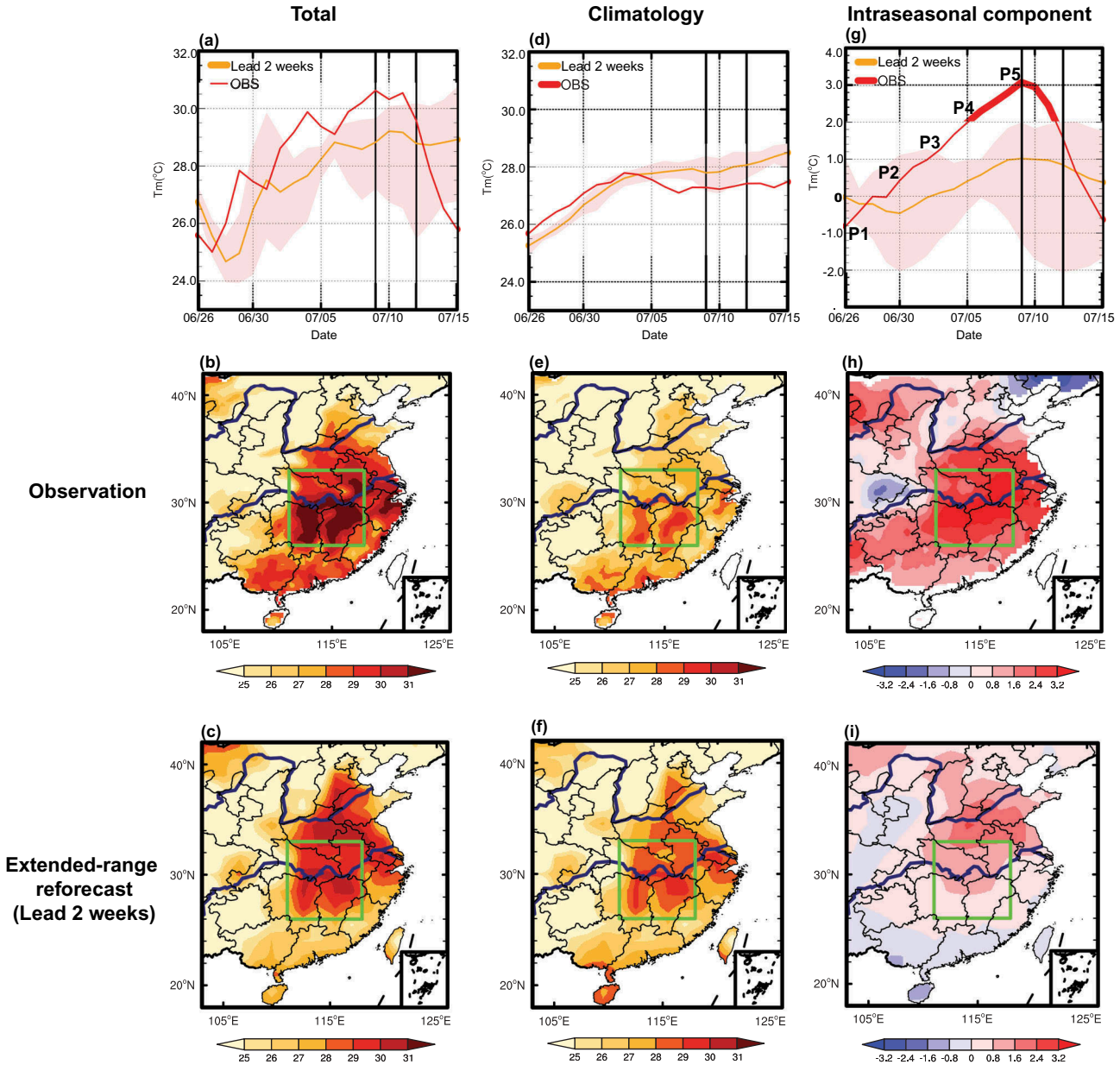

Figure 1. (a) Time series of the T_m (units: °C) averaged over the YRV in summer 2012 for the observation (red line), the ensemble mean (orange line), and the ensemble members (shaded). (b) Observed and (c) extended-range reforecast temporal-averaged T_m (shading; units: °C) during the heatwave event (9–12 July). The green boxes denote the location of the YRV. Panels (d–f) and (g–i) are the same as (a–c) but for the climatology and the intraseasonal timescales, respectively. P = Phase.

are not attributable to the climatological bias of the reforecast system.

Given the adverse effect of the climatological biases and the close relationship between the intraseasonal components and the heatwave event, the climatological components are removed and the contribution of the intraseasonal component is investigated. In accordance with the ISO life cycle (see details in Qi et al. (2019)), the warming process in this heatwave event is defined as the period from phase 1 to phase 5 (26 June to 12 July). As shown in Figure 1(g–i), during the warming process associated with the heatwave, there are large biases in the reforecast compared to the observation along with the local intraseasonal variation. In the observation, the warming amplitude reaches 6°C (31°C minus 25°C; see Figure 1(a)), while the ISO-related warming is 3.9°C (red line in Figure 1(g)), as measured by the T_m difference between phase 1 and phase 5, which accounts for nearly 70% of the warming amplitude. That is, the ISO-related warming is the major contributor to the local warming process over the YRV.

However, the reforecast ISO-associated warming from phase 1 to phase 5 is only 1.5°C, which is only one third of the observed (orange line in Figure 1(g)). Moreover, the warming center moves significantly northward from the YRV region to the Yellow River Valley region, which obviously contributes to the location bias (northward shift) of this heatwave prediction. Therefore, the reforecast biases of both amplitude and location associated with this heatwave are primarily attributable to the biases of the local intraseasonal component in the extended-range forecast.

3.2 Role of ISO in the extended-range prediction of the HW event

We further examine whether the local biases of the intraseasonal component are associated with remotely propagating intraseasonal waves. First, the evolutions of the intraseasonal vorticity and circulations from the tropics are shown in Figure 2. In the observation (Figure 2(a)), a meridional dipole anomaly over the tropical western Pacific features an anomalous cyclone to the south between 10° and 20°N and an anomalous anticyclone to the north between 20° and 30°N, and persistently migrates westward from phase 1 to phase 5. The anticyclonic anomaly begins to affect the YRV from phase 3, and its center is located to the south of the local region in phase 5. In contrast, the meridional dipole pattern and its westward propagation are predicted well with a two-week lead, although the anticyclonic center shifts northwards, particularly during the late period of the warming, compared with the observation.

Furthermore, we examine the heatwave-associated evolutions of the intraseasonal propagation from the extratropical region, as shown in Figure 3. In the observation (Figure 3(a)), during the early period of heatwave development (phases 1–3), an eastward migratory wave train from Eastern Europe to the Okhotsk Sea can be well detected. Along with the intraseasonal traveling wave train, an anomalous anticyclone that is located over the northeast of Lake Balkhash (~50°N, 85°E) in phase 1, propagates gradually southeastwards from the west Siberian Plain to the YRV longitudes from phase 1 to phase 3. During the late period of heatwave development (phases 4–5), the anticyclonic anomaly arrives at the YRV and transports negative vorticity advection to the local region (Qi et al. 2019), which is beneficial for generating the anomalous subsidence dynamically in the upper troposphere (Ren, Liu, and Wu 2007; Ren and Wu 2003). Accompanied by the eastward extension of the South Asian high (SAH), a strong high-pressure anomaly is well established over the YRV eventually, corresponding to the onset of the heatwave.

However, in the reforecast, the eastward-migrating intraseasonal wave train cannot be well reproduced (Figure 3(b)). The wave train propagating from Eastern Europe to the Okhotsk Sea can be predicted in the first two phases, but its intensity weakens rapidly to the east of the Okhotsk Sea after phase 3. Even though the key anticyclonic anomaly in the wave train is visible in the reforecast during the early period of heatwave development, it vanishes in phase 3 such that it cannot provide the negative vorticity advection to the YRV during the late period, which hinders the formation of the strong high-pressure anomaly. Accordingly, the SAH does not exhibit an eastward extension in the reforecast either. Therefore, the inaccurate reforecast of the ISO signal from the extratropical region leads to the absence of the important strong high-pressure anomaly over the YRV, resulting in the evident underestimation of the warming over the local region and the ultimate disappearance of the heatwave event.

4. Summary and discussion

Based on the ECMWF's S2S reforecast database, this study evaluates the extended-range prediction performance of a typical ISO-associated heatwave event over the YRV. Our previous work (Qi et al. 2019) reported the crucial effect of extratropical ISOs on the heatwave generation in the observation, and this follow-up work further verifies its essential role in the occurrence of the heatwave in the extended-range prediction. As a result, the reforecast temperature is evidently underestimated at a two-week lead time, and this heatwave event fails to occur in the reforecast. Further analysis reveals that, rather than the climatological bias of the reforecast system, the biases from the extratropical ISO signal in the reforecast contribute the most to the failure of the heatwave occurrence. Specifically, due to the absence of the intraseasonal signal along with the eastward propagating wave train in the reforecast, the key strong high-pressure anomaly over the YRV that causes the heatwave in the observation cannot be reproduced in the reforecast, which ultimately results in the failure to predict this heatwave event. This study indicates that accurately predicting extratropical intraseasonal signals from the Eurasian continent is potentially important for the extended-range prediction of extreme heatwave events over East Asia.

The cause of the evident damping of the extratropical intraseasonal signal in the extended-range prediction is worthy of further investigation. Note that the source and the propagation area of extratropical intraseasonal wave trains are located over Eurasia, and the surface condition and its land–atmosphere interactions may play a crucial

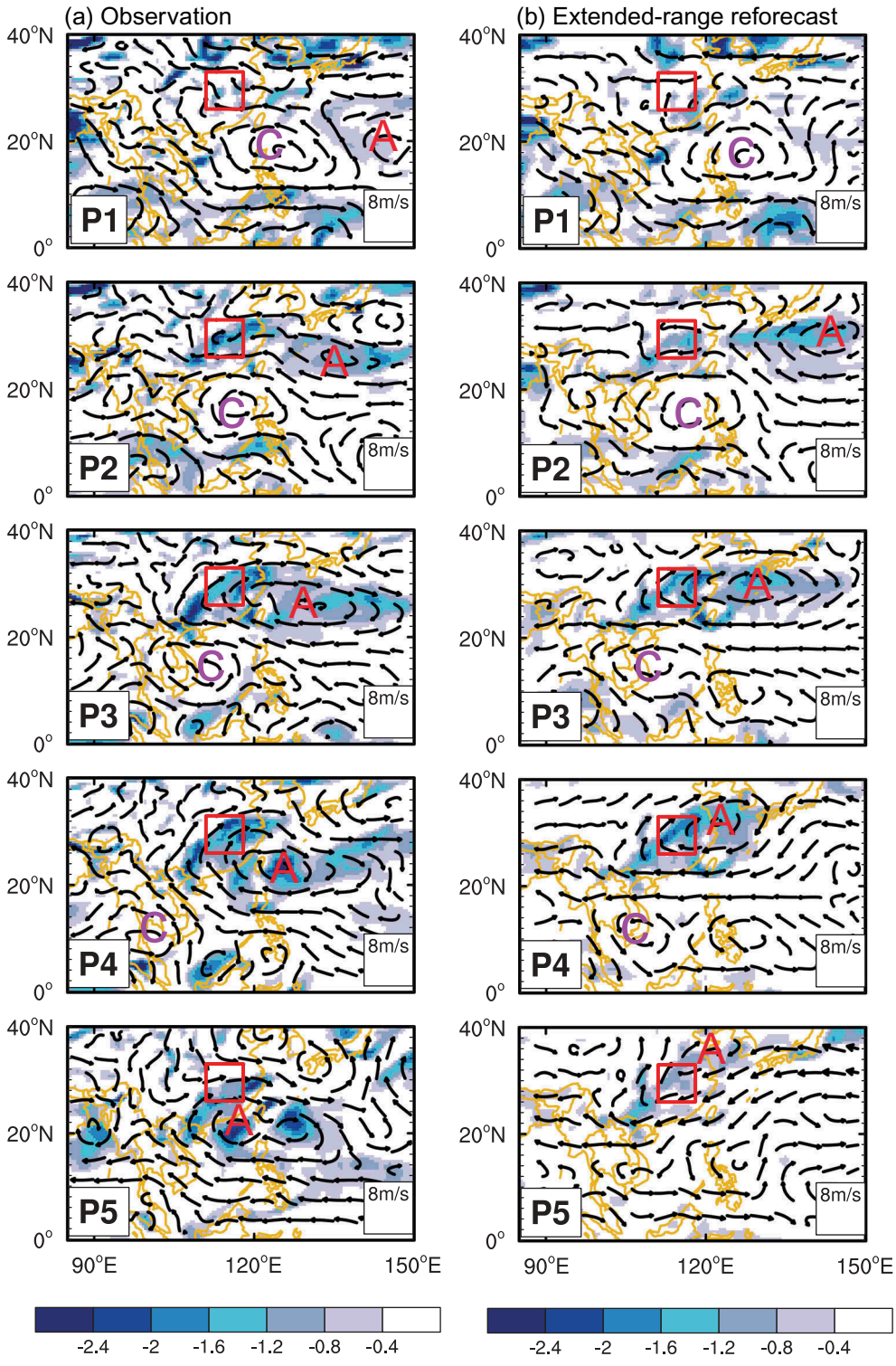

Figure 2. Temporal evolution of 850 hPa rotational wind (vectors; units: m s^{-1}) and vorticity (shading; units: 10^{-6} s^{-1}) anomalies on the intraseasonal time scale for the (a) observation and (b) extended-range reforecast during the period of heatwave development. 'A' and 'C' denote the centers of the anticyclonic and cyclonic anomalies, respectively. The red boxes represent the core region of the YRV. P = phase.

role in extended-range forecasts of intraseasonal perturbations. Previous studies have reported that the relatively slow but predictable varying signals of the land should be taken into account when initializing a prediction (Shukla and Kinter 2006), such as the soil moisture/temperature anomaly (e.g. Fischer et al. 2007; Koster et al. 2010), land cover (Findell et al. 2017), snow cover (Li et al. 2018), sea ice (Wu and Jennifer 2019), and even the

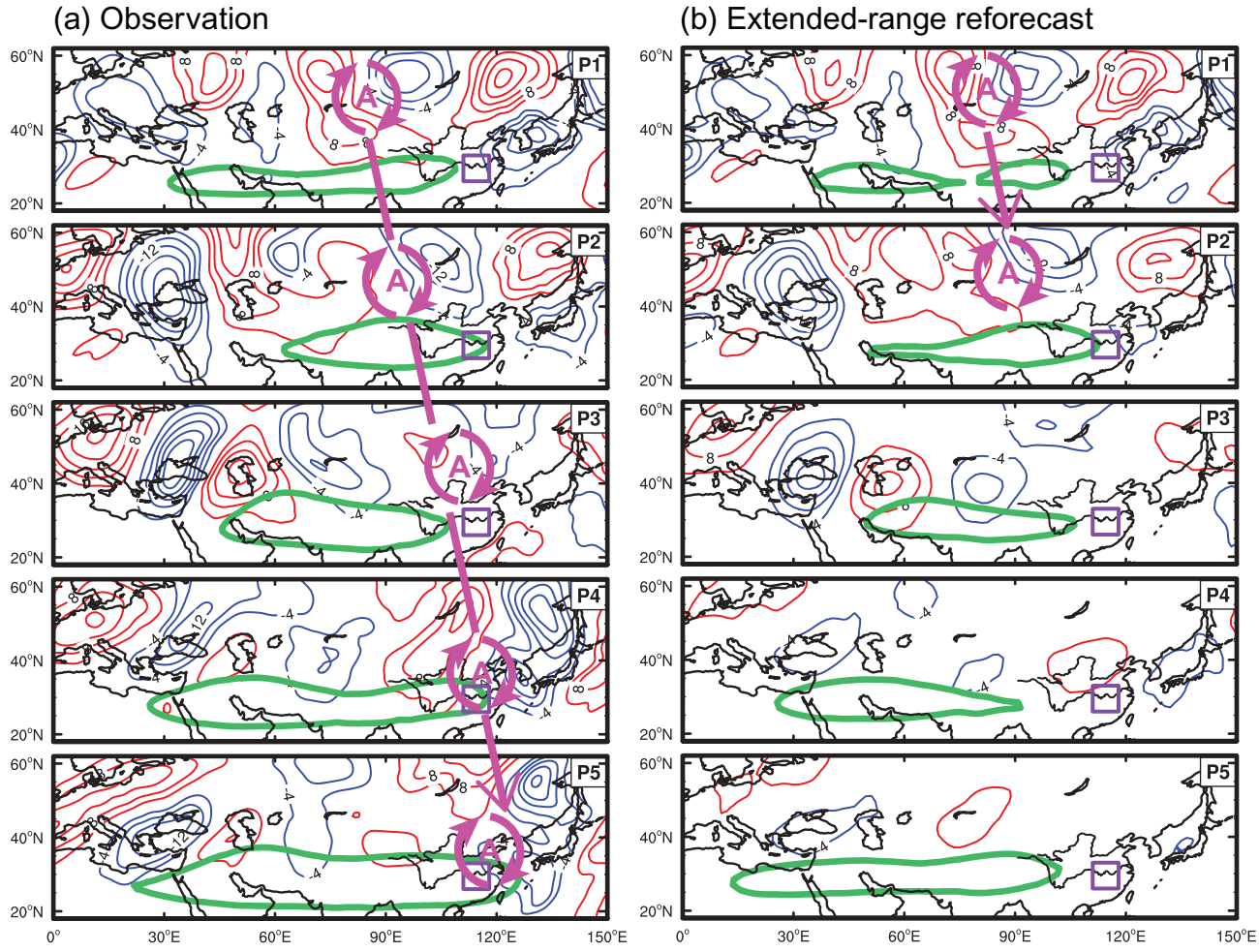

Figure 3. Temporal evolution of 200 hPa meridional wind anomalies (contours; units: gpm) on the intraseasonal time scale for the (a) observation and (b) extended-range reforecast during the period of heatwave development. Green lines are the 200 hPa geopotential height contours at 12,540 gpm representing the location of the SAH. 'A' denotes the center of the anticyclonic anomalies. The purple boxes represent the core region of the YRV. P = phase.

urbanization (Wang et al. 2017). Moreover, mountain torques play essential roles in atmospheric oscillations (Lott, Robertson, and Ghil 2003), but may not be reflected appropriately in prediction systems. The above two aspects form part of our ongoing studies. Optimizing the land–atmosphere interaction may facilitate a better extended-range prediction performance of the midlatitude wave trains, and therefore improve sub-seasonal predictions of extreme heatwave events over East Asia.

Disclosure statement

No potential conflict of interest was reported by the authors.

Funding

This study was supported by the National Key R&D Program of China (Grant No. 2018YFC1505903), the National Natural Science Foundation of China (Grant No. 41775071), and the National Key R&D Program of China (Grant No. 2016YFA0602401).

References

Anderson, G. B., and M. L. Bell. 2011. "Heat Waves in the United States: Mortality Risk during Heat Waves and Effect Modification by Heat Wave Characteristics in 43 U.S. Communities." *Environmental Health Perspectives* 119: 210–218. doi:10.1289/ehp.1002313.

Chen, R.-D., Z.-P. Wen, and R.-Y. Lu. 2018. "Large-scale Circulation Anomalies and Intraseasonal Oscillations Associated with Long-lived Extreme Heat Events in South China." *Journal of Climate* 31: 213–232. doi:10.1175/JCLI-D-17-0232.1.

Chen, Y., and P.-M. Zhai. 2017. "Simultaneous Modulations of Precipitation and Temperature Extremes in Southern Parts of China by the Boreal Summer Intraseasonal Oscillation." *Climate Dynamics* 49: 3363–3381. doi:10.1007/s00382-016-3518-4.

Dee, D. P., S. M. Uppala, A. J. Simmons, P. Berrisford, P. Poli, S. Kobayashi, U. Andrae, et al. 2011. "The ERA-Interim Reanalysis: Configuration and Performance of the Data Assimilation System." *Quarterly Journal of the Royal Meteorological Society* 137: 553–597. doi:10.1002/qj.828.

Findell, K. L., A. Berg, P. Gentine, J. P. Krasting, B. R. Lintner, S. Malyshev, J. A. Santanello, and E. Shevliakova. 2017. "The Impact of Anthropogenic Land Use and Land Cover Change on Regional Climate Extremes." *Nature Communications* 8: 989. doi:10.1038/s41467-017-01038-w.

Fischer, E. M., S. I. Seneviratne, D. Lüthi, and C. Schär. 2007. "Contribution of Land-atmosphere Coupling to Recent European Summer Heat Waves." *Geophysical Research Letters* 34: L06707. doi:10.1029/2006GL029068.

Gao, M.-N., J. Yang, B. Wang, S.-Y. Zhou, D.-Y. Gong, and S. J. Kim. 2018. "How are Heat Waves over Yangtze River Valley Associated with Atmospheric Quasi-biweekly Oscillation?" *Climate Dynamics* 51: 4421–4437. doi:10.1007/s00382-017-3526-z.

Hsu, P.-C., J. Y. Lee, K. J. Ha, and C.-H. Tsou. 2017. "Influences of Boreal Summer Intraseasonal Oscillation on Heat Waves in Monsoon Asia." *Journal of Climate* 30: 7191–7211. doi:10.1175/JCLI-D-16-0505.1.

Huang, W., H.-D. Kan, and S. Kovats. 2010. "The Impact of the 2003 Heat Wave on Mortality in Shanghai, China." *Science of the Total Environment* 408: 2418–2420. doi:10.1289/ehp.1103532.

Koster, R. D., S. P. P. Mahanama, T. J. Yamada, G. Balsamo, A. A. Berg, M. Boisserie, P. A. Dirmeyer, et al. 2010. "Contribution of Land Surface Initialization to Subseasonal Forecast Skill: First Results from a Multi-model Experiment." *Geophysical Research Letters* 37: L02402. doi:10.1029/2009GL041677.

Li, W.-K., W.-D. Guo, B. Qiu, Y.-K. Xue, P.-C. Hsu, and J.-F. Wei. 2018. "Influence of Tibetan Plateau Snow Cover on East Asian Atmospheric Circulation at Medium-range Time Scales." *Nature Communications* 9: 1. doi:10.1038/s41467-018-06762-5.

Lott, F., A. W. Robertson, and M. Ghil. 2003. "Mountain Torques and Northern Hemisphere Low-Frequency Variability. Part II: Regional Aspects." *Journal of the Atmospheric Sciences* 61: 1272–1283. doi:10.1175/1520-0469(2004)061<1272:MTANHL>2.0.CO;2.

Mariotti, A., P. M. Ruti, and M. Rixen. 2018. "Progress in Subseasonal to Seasonal Prediction through a Joint Weather and Climate Community Effort." *Npj Climate and Atmospheric Science* 1: 4. doi:10.1038/s41612-018-0014-z.

Qi, X., J. Yang, M.-N. Gao, H.-W. Yang, and H.-B. Liu. 2019. "Roles of the Tropical/extratropical Intraseasonal Oscillations on Generating the Heat Wave over Yangtze River Valley: A Numerical Study." *Journal of Geophysical Research: Atmospheres* 124: 3110–3123. doi:10.1029/2018JD029868.

Ren, R. C., Y. M. Liu, and G. X. Wu. 2007. "Impact of South Asia High on the Short-term Variation of the Subtropical Anticyclone over Western Pacific in July 1998." *Acta Meteorologica Sinica* 65 (2): 183–197. [in Chinese]. doi:10.1002/jrs.1570.

Ren, R. C., and G. X. Wu. 2003. "On the Short-term Structure and Formation of the Subtropical Anticyclone in the Summer of 1998." *Acta Meteorologica Sinica* 61 (2): 180–195. [in Chinese]. doi:10.1007/BF02948883.

Shukla, J., and J. L. Kinter III. 2006. "Predictability of Seasonal Climate Variations." In *Predictability of Weather and Climate*, edited by T. Palmer and R. Hagedom, 306–341. Cambridge: Cambridge Univ. Press. Chap. 12.

Simmons, A., S. Uppala, D. Dee, and S. Kobayashi. 2007. "ERA-Interim: New ECMWF Reanalysis Products from 1989 Onwards." *ECMWF Newsletter* 110: 25–35. doi:10.21957/pocnex23c6.

Teng, H.-Y., G. Branstator, H. Wang, G. A. Meehl, and W. M. Washington. 2013. "Probability of US Heat Waves Affected by a Subseasonal Planetary Wave Pattern." *Nature Geoscience* 6: 1056–1061. doi:10.1038/ngeo1988.

Vitart, F., C. Ardilouze, A. Bonet, A. Brookshaw, M. Chen, C. Codorean, M. Déqué, et al. 2017. "The Subseasonal to Seasonal (S2S) Prediction Project Database." *Bulletin of the American Meteorological Society* 98: 163–173. doi:10.1175/BAMS-D-16-0017.1.

Wang, J., Z.-W. Yan, X.-W. Quan, and J.-M. Feng. 2017. "Urban Warming in the 2013 Summer Heat Wave in Eastern China." *Climate Dynamics* 48: 3015–3033. doi:10.1007/s00382-016-3248-7.

Wu, B.-Y., and A. F. Jennifer. 2019. "Summer Arctic Cold Anomaly Dynamically Linked to East Asian Heat Waves." *Journal of Climate* 32: 1137–1150. doi:10.1175/JCLI-D-18-0370.1.

Wu, J., and X.-J. Gao. 2013. "A Gridded Daily Observation Dataset over China Region and Comparison with the Other Datasets." *Chinese Journal of Geophysics* 56: 1102–1111. [in Chinese]. doi:10.6038/cjg20130406.

Xu, Y., X.-J. Gao, Y. Shen, C.-H. Xu, Y. Shi, and F. Giorgi. 2009. "A Daily Temperature Dataset over China and Its Application in Validating A RCM Simulation." *Advances in Atmospheric Sciences* 26: 763–772. doi:10.1007/s00376-009-9029-z.

Yang, J., Q. Bao, B. Wang, D.-Y. Gong, H.-Z. He, and M.-N. Gao. 2014. "Distinct Quasi-biweekly Features of the Subtropical East Asian Monsoon during Early and Late Summers." *Climate Dynamics* 42: 1469–1486. doi:10.1007/s00382-013-1728-6.

Yang, J., B. Wang, and Q. Bao. 2010. "Biweekly and 21-30-day Variations of the Subtropical Summer Monsoon Rainfall over the Lower Reach of the Yangtze River Basin." *Journal of Climate* 23: 1146–1159. doi:10.1175/2009JCLI3005.1.

Zhu, Z.-W., and T. Li. 2018. "Extended-range Forecasting of Chinese Summer Surface Air Temperature and Heat Waves." *Climate Dynamics* 50: 2007–2021. doi:10.1007/s00382-017-3733-7.